Article

1-(1-Naphthyl)Ethylamine Adsorption on Platinum Surfaces: On the Mechanism of Chiral Modification in Catalysis

Ilkeun Lee, Zhen Ma, Shinji Kaneko, and Francisco Zaera

J. Am. Chem. Soc., **2008**, 130 (44), 14597-14604 • DOI: 10.1021/ja803667v • Publication Date (Web): 11 October 2008

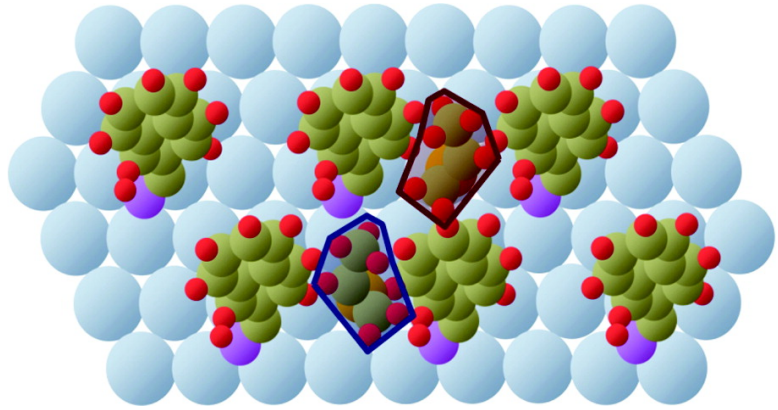

J|A|C|S
ARTICLES

Published on Web 10/11/2008

1-(1-Naphthyl)Ethylamine Adsorption on Platinum Surfaces: On the Mechanism of Chiral Modification in Catalysis

Ilkeun Lee, Zhen Ma,† Shinji Kaneko, and Francisco Zaera*

Department of Chemistry, University of California, Riverside, California 92521

Received May 16, 2008; E-mail: zaera@ucr.edu

Abstract: The adsorption of 1-(1-naphthyl)ethylamine (NEA) on platinum surfaces has been characterized by reflection−absorption infrared spectroscopy (RAIRS) and temperature-programmed desorption (TPD) both under ultrahigh vacuum and in situ from liquid solutions. The main focus of this study was to identify the mechanism by which single enantiomers of NEA bestow chirality on the platinum surface. Evidence was acquired for both of the prevailing explanations available in the literature for the NEA behavior: formation of supramolecular chiral templates and complexation of individual modifiers with the reactant. Indeed, TPD titrations of NEA-modified Pt(111) using propylene oxide (PO) as a chiral probe point to a relative enhancement in the adsorption of one enantiomer over the other at intermediate NEA coverages, which is the behavior expected from the templating mechanism. However, a difference in adsorption energetics was also observed. Both the TPD and RAIRS data suggest possible interactions between the adsorbed NEA and adjacent PO that differ according to the relative chirality of the two compounds. The NEA uptake from solution displays additional enantioselectivity, in particular when the adsorption of enantiopure compounds is compared with that of racemic mixtures, and also points to possible adsorption changes induced by ethyl pyruvate, a common reactant in chiral hydrogenation processes.

1. Introduction

In view of the increasing prominence of chiral synthesis in the pharmaceutical and agro industries,[1,2] it would be highly desirable to develop enantioselective processes that use heterogeneous catalysts. Heterogeneous catalysts are in general easier to handle and separate than are the homogeneous counterparts employed nowadays in many applications, and their use would make such industrial processes cheaper and greener. Unfortunately, there are to date no viable heterogeneous enantioselective catalysts available for practical uses; the promise of using heterogeneous catalysis for manufacturing chiral molecules remains in the future.[3]

One of the most viable approaches for enantioselective heterogeneous catalysis is via the use of chiral modifiers. Two examples of this have been advanced in the literature so far: the hydrogenation of β-ketoesters using tartaric acid-modified nickel catalysts[4,5] and the hydrogenation of α-ketoesters using platinum catalysts modified by cinchona alkaloids.[6,7] A few variations of these have been reported, but their extension to other more general systems has not yet been possible.[8−10] Furthermore, the two known cases have been explained by significantly different mechanisms.[11] On the one hand, each individual molecule of the cinchona alkaloids is believed to possess all of the ingredients needed to impart chirality to catalytic reactions by itself, and it may form a complex with the reactant on the surface of the catalyst in such a way as to force a specific adsorption geometry and leads to the selective hydrogenation of one of the two faces of the prochiral carbonyl group.[12−15] In fact, cinchona alkaloids are also chiral promoters in several homogeneous reactions, without the intervention of any surfaces.[16] In contrast, tartaric acid, which is a much simpler molecule, may not be able to individually promote such 1:1 interactions. Instead, it has been suggested that tartaric acid may form supramolecular chiral structures on the surface with chiral pockets where the catalysis may take place.[17,18] This ordering may be local, since long-range ordered structures are in general not observed in these systems.[19,20] Moreover, the formation of chiral surface sites requires bonding of the modifier to the

† Present address: Chemical Sciences Division, Oak Ridge National Laboratory, Oak Ridge, TN 37831.

(1) Blaser, H. U.; Spindler, F.; Studer, M. *Appl. Catal., A* **2001**, *221*, 119.
(2) Thayer, A. M. *Chem. Eng. News* **2007**, *85* (32), 11.
(3) Murzin, D.; Mäki-Arvela, P.; Toukoniitty, E.; Salmi, T. *Catal. Rev.* **2005**, *47*, 175.
(4) Isoda, T.; Ichikawa, A.; Shimamoto, T. *Rikagaku Kenkyusho Hokoku* **1958**, *34*, 134.
(5) Izumi, Y. *Adv. Catal.* **1983**, *32*, 215.
(6) Orito, Y.; Imai, S.; Niwa, S. *Nippon Kagaku Kaishi* **1980**, 670.
(7) Webb, G.; Wells, P. B. *Catal. Today* **1992**, *12*, 319.
(8) Studer, M.; Blaser, H. U.; Exner, C. *Adv. Synth. Catal.* **2003**, *345*, 45.
(9) Bartók, M. *Curr. Org. Chem.* **2006**, *10*, 1533.
(10) Mallat, T.; Orglmeister, E.; Baiker, A. *Chem. Rev.* **2007**, *107*, 4863.
(11) Zaera, F. *J. Phys. Chem. C* **2008**, ASAP (DOI: 10.1021/jp804588v).
(12) Burgi, T.; Baiker, A. *Acc. Chem. Res.* **2004**, *37*, 909.
(13) Vayner, G.; Houk, K. N.; Sun, Y.-K. *J. Am. Chem. Soc.* **2004**, *126*, 199.
(14) Lavoie, S.; Laliberté, M.-A.; Temprano, I.; McBreen, P. H. *J. Am. Chem. Soc.* **2006**, *128*, 7588.
(15) Ma, Z.; Zaera, F. In *Design of Heterogeneous Catalysis: New Approaches Based on Synthesis, Characterization, and Modelling*; Ozkan, U. S., Ed.; Wiley-VCH: Weinheim, Germany, 2008 (in press).
(16) Hoffmann, H. M. R.; Frackenpohl, J. *Eur. J. Org. Chem.* **2004**, 4293.
(17) Raval, R. *CATTECH* **2001**, *5*, 12.
(18) Osawa, T.; Harada, T.; Takayasu, O. *Curr. Org. Chem.* **2006**, *10*, 1513.
(19) Humblot, V.; Haq, S.; Muryn, C.; Hofer, W. A.; Raval, R. *J. Am. Chem. Soc.* **2002**, *124*, 503.
(20) Jones, T. E.; Baddeley, C. J. *Surf. Sci.* **2002**, *513*, 453.

surface via two or more points within each molecule[17,18] and perhaps also a cooperative interaction between the adsorbed tartrate and β-ketoester species.[21] Regardless, it appears that the lack of complexity of the individual chiral modifier in this case must be compensated by the intervention of several molecules in the chiral templating process. In thermodynamic terms, the dichotomy between the two proposed models can be viewed as a balance between enthalpic and entropic factors being the ones controlling the chiral modification. In order to be able to design new chirality-bestowing systems, it would be highly desirable to develop a more unified model in which both those factors are considered.

In this report, we summarize the key results deriving from our surface-science studies of the adsorption of 1-(1-naphtyl)-ethylamine (NEA) on platinum surfaces. NEA is a chiral molecule capable of inducing a modest degree of enantioselectivity to the hydrogenation of α-ketoesters using platinum catalysts.[22] It possesses some of the features responsible for chiral modification in cinchona alkaloids, including a chiral center directly bonded to an aromatic ring that facilitates adsorption, but it is also a much simpler molecule, unable to adopt the three-dimensional chiral configurations seen with the cinchona. Therefore, it could be argued that NEA may not be able to impart chirality solely by formation of 1:1 complexes with the reactant; a degree of supramolecular cooperation may play a part in chiral modification by this molecule. This is a case of a molecule that may require both templating and individual complexation mechanisms to bestow chirality to surfaces.

Our data suggest that this may indeed be the case. On one hand, it was determined that adsorption of either enantiomer of NEA on single-crystal Pt(111) surfaces under ultrahigh vacuum (UHV) leads to an enhancement in the extent of the uptake of one enantiomer of propylene oxide (PO), a chiral probe, over the other. This type of behavior has been previously seen with 2-butanol,[23−25] 2-methylbutanoic acid,[26,27] and a number of amino acids[28] on Pt(111) and Pd(111) surfaces and is likely to originate from a collective effect of the adsorbed layer of the modifier rather than from individual interactions with the second adsorbate.[29] On the other hand, enantioselectivity in this case is also manifested by a change in the energetics of the desorption of PO from the NEA-modified surface. Reflection−absorption infrared spectroscopy (RAIRS) results on the NEA + PO coadsorbed systems suggest some degree of interaction between the two molecules on the surface.

In separate studies, the adsorption of NEA from liquid solutions onto a polished platinum disk was characterized in situ by RAIRS. Differences in the binding geometries of the surface NEA species were identified, in particular between enantiopure and racemic adsorbates, suggesting some chiral intermixing and a degree of intermolecular interactions on the surface. Infrared data from surfaces having ethyl pyruvate adsorbed on NEA-precovered platinum are also consistent with some degree of intermolecular interaction in that case.

2. Experimental Section

The temperature-programmed desorption (TPD) and RAIRS UHV experiments reported here were carried out in a two-level chamber described in more detail elsewhere.[30,31] Briefly, the entire system was cryopumped to a base pressure of less than 3×10^{-10} Torr. The TPD experiments were carried out in the main level using a UTI 100C quadrupole mass spectrometer retrofitted with a retractable nose cone ending in a 5 mm diameter aperture for the selective detection of the desorbing molecules. A constant heating rate of 10 K/s was used in all of the TPD runs, and a bias voltage of −100 V was applied to the crystal in order to repel any stray electrons.[32,33] The RAIRS experiments were carried out in the second level of the UHV apparatus, which can be reached by a long-travel manipulator. The IR beam from a Bruker Equinox 55 FT-IR spectrometer was sequentially directed through a polarizer within a purged volume (set to shine p-polarized light on the surface) and into the UHV chamber through a NaCl window, focused onto the sample at grazing incidence (∼85°), sent back to the atmospheric side through a second NaCl window, and focused onto a mercury−cadmium−telluride (MCT) detector.[34] Spectra were collected by averaging 2000 scans taken with 4 cm^{-1} resolution and ratioed against spectra obtained in a similar way for the clean surface prior to any gas dosing. The Pt(111) single crystal used in the UHV experiments was mounted on the long-travel manipulator, which can be cooled to ∼80 K and resistively heated to 1100 K. The temperature of the crystal was measured using a chromel−alumel thermocouple spot-welded to its side. The surface was routinely cleaned by cycles of oxidation in 2×10^{-6} Torr of oxygen at 700 K and annealing in vacuum at 1100 K, and occasionally by Ar^+ sputtering although this latter procedure was minimized to avoid the creation of surface defects. Gas exposures were performed by backfilling of the vacuum chamber and are reported in langmuirs (1 langmuir ≡ 10^{-6} Torr·s) without correction for differences in ion-gauge sensitivities. Gas dosing was done at temperatures below 100 K unless otherwise indicated.

The experimental setup used for the in situ RAIRS characterization of liquid−solid interfaces has also been described in detail in previous publications.[35−37] Briefly, a polished polycrystalline Pt disk mounted on a micrometer-driven supporting rod was cleaned before each experiment by repeated electrochemical oxidation−reduction cycles, flushed with a neat solvent (CCl_4 in this report) to record the background spectra, and reduced by bubbling hydrogen.[38] Spectra for both the adsorbate and the clean surface were obtained by pressing the Pt disk against a CaF_2 prism (cut in a trapezoidal shape with two faces beveled at 60°) in order to pass the infrared beam from a Mattson Sirius 100 FT-IR spectrometer equipped with a MCT detector into and out of the liquid thin film present above the surface. The reported RAIRS data were obtained by first dividing the trace obtained using p-polarized light by that for s-polarized light with the solution of interest, and then ratioing that p/s data against the corresponding p/s background data obtained with the pure solvent. All of the reported spectra in these experiments correspond to averages from 512 scans taken with 4

(21) Jones, T. E.; Baddeley, C. J. *Surf. Sci.* **2002**, *519*, 237.
(22) Minder, B.; Schuerch, M.; Mallat, T.; Baiker, A.; Heinz, T.; Pfaltz, A. *J. Catal.* **1996**, *160*, 261.
(23) Stacchiola, D.; Burkholder, L.; Tysoe, W. T. *J. Am. Chem. Soc.* **2002**, *124*, 8984.
(24) Lee, I.; Zaera, F. *J. Phys. Chem. B* **2005**, *109*, 12920.
(25) Gao, F.; Wang, Y.; Li, Z.; Furlong, O.; Tysoe, W. T. *J. Phys. Chem. C* **2008**, *112*, 3362.
(26) Stacchiola, D.; Burkholder, L.; Zheng, T.; Weinert, M.; Tysoe, W. T. *J. Phys. Chem. B* **2005**, *109*, 851.
(27) Lee, I.; Zaera, F. *J. Am. Chem. Soc.* **2006**, *128*, 8890.
(28) Burkholder, L. A.; Stacchiola, D. J.; Tysoe, W. T. *Abstr. Pap.−Am. Chem. Soc.* **2004**, *228*, COLL U474.
(29) Romá, F.; Stacchiola, D.; Zgrablich, G.; Tysoe, W. T. *J. Chem. Phys.* **2003**, *118*, 6030.
(30) Lee, I.; Zaera, F. *J. Phys. Chem. B* **2005**, *109*, 2745.
(31) Morales, R.; Zaera, F. *J. Phys. Chem. C* **2007**, *111*, 18367.
(32) Zaera, F.; Chrysostomou, D. *Surf. Sci.* **2000**, *457*, 89.
(33) Lee, I.; Zaera, F. *J. Phys. Chem. C* **2007**, *111*, 10062.
(34) Zaera, F.; Chrysostomou, D. *Surf. Sci.* **2000**, *457*, 71.
(35) Zaera, F. *Int. Rev. Phys. Chem.* **2002**, *21*, 433.
(36) Kubota, J.; Ma, Z.; Zaera, F. *Langmuir* **2003**, *19*, 3371.
(37) Ma, Z.; Lee, I.; Zaera, F. *J. Am. Chem. Soc.* **2007**, *129*, 16083.
(38) Ma, Z.; Kubota, J.; Zaera, F. *J. Catal.* **2003**, *219*, 404.

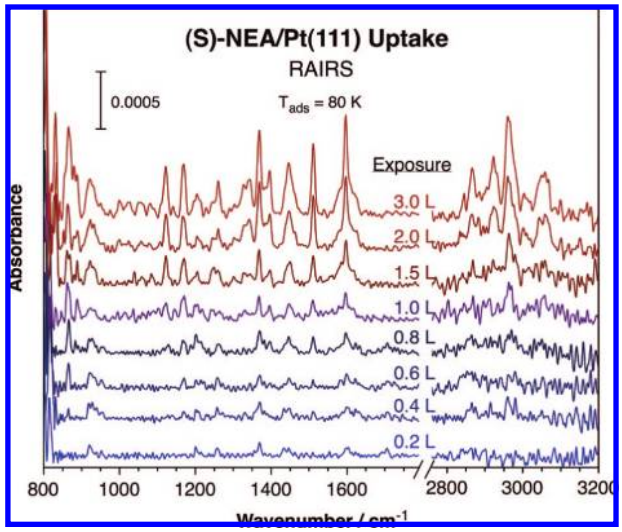

Figure 1. RAIRS for (*S*)-NEA adsorbed on a single-crystal Pt(111) surface at 80 K under UHV as a function of initial exposure. The vibrational assignments are provided in Table 1. Changes in adsorption geometry are manifested by changes in the spectra around 0.4 and 1.0 L.

cm^{-1} resolution. All of these experiments were carried out at ambient temperature (295 ± 2 K).

The (*R*)-(+)-, (*S*)-(−)-, and racemic (±)-NEA (99, 99, and 98% purity, respectively) and the (*R*)- and (*S*)-PO (both 99% purity) were all purchased from Aldrich, purified via repeated freeze−pump−thaw vacuum distillations before use, and checked in situ by mass spectrometry. The carbon tetrachloride solvent (99.9% purity) was also obtained from Aldrich, and the H_2 gas (99.999% purity) was supplied by Liquid Carbonic; both were used as received.

3. Results and Discussion

3.1. Low-Temperature Uptake of NEA on Pt(111) under Vacuum. The uptake of NEA on clean Pt(111) surfaces under vacuum and at liquid nitrogen temperatures was characterized first. The RAIRS data obtained for (*S*)-NEA as a function of initial exposure is reported in Figure 1; similar results were obtained for the (*R*) enantiomer and also for both commercially purchased and made-in-house racemic mixtures (Figures S1, S2, and S3, respectively, in the Supporting Information). The vibrational assignments of the peaks seen in these data, which were made with the help of reported studies of naphthalene,[39,40] substituted naphthalenes,[41,42] and ethylamine[43] and also based on comparisons with our previous data for cinchona alkaloids,[44,45] are summarized in Table 1. Our results are somewhat different both in terms of peak positions and peak intensities from those published previously by McBreen and co-workers[46] but correlate well with the molecular characteristics of NEA.

The first thing to notice from these RAIRS is the fact that the positions of the peaks for the adsorbed NEA closely match those for the pure liquid. This means that adsorption is molecular, at least at these low temperatures, and that it occurs with minimal molecular distortion. On the other hand, three distinct regimes can be identified during the uptake, manifested primarily by changes in the relative intensities of the different vibrational features. The variations in the spectra reflect changes in adsorption geometry, because, according to the surface selection rule that applies to RAIRS on metals, only the component of the vibrational dynamic dipoles oriented perpendicular to the surface is active for infrared absorption on those surfaces.[35,47] On the basis of this rule, different definite adsorption geometries can be identified for NEA on Pt(111) for exposures below 0.4 L, between 0.4 and 1.0 L, and above 1.0 L.

At low coverages, for exposures below 0.4 L, the main vibrational modes apparent in the RAIRS traces are those at 920, 1200, 1257, 1369, 1432, 1448, and 1600 cm^{-1}, which correspond, respectively, to rocking of the methyl group [$\rho(CH_3)$], in-plane deformations of the C−H bonds of the substituted and nonsubstituted sides of the aromatic ring [$\delta_{ip}(CH)_{ring\text{-}s}$ and $\delta_{ip}(CH)_{ring\text{-}n}$, respectively], the symmetric (umbrella) and asymmetric deformations of the methyl moiety [$\delta_s(CH_3)_{EtNH_2}$ and $\delta_a(CH_3)_{EtNH_2}$, respectively (two modes for the latter)], and an in-plane naphthalene ring symmetric deformation with a dynamic dipole along the ring's short axis [$\delta_{ip}(CC)_{ring\text{-}y}$]. This indicates adsorption with the naphthalene ring standing up along its short axis on the surface, that is, bonded through its long side. There is a possibility that bonding occurs with participation of the lone pair of the nitrogen atom.

Exposure of the surface to additional NEA leads to the development of a few new RAIRS peaks, noticeably those at 865, 928, 1168, 1257, and 1620 cm^{-1}. The respective assignments of these peaks are as follows: three out-of-plane C−H deformations, two in the nonsubstituted moiety of the naphthalene ring [$\delta_{oop}(CH)_{ring\text{-}n}$] and one in its substituted side [$\delta_{oop}(CH)_{ring\text{-}s}$], an in-plane C−H deformation in the nonsubstituted section of the ring [$\delta_{ip}(CH)_{ring\text{-}n}$], and an in-plane skeletal deformation of the ring [$\nu_{ip}(CC)_{ring}$]. Clearly, a new adsorption arrangement develops at this point, with the aromatic ring somewhat tilted away from the surface normal. On the other hand, there is no detectable signal for the in-plane CH deformation [$\delta_{ip}(CH)_{ring\text{-}n}$] at 1121 cm^{-1}, and only a low-intensity peak for the in-plane ring deformation [$\nu_{ip}(CC)_{ring\text{-}x}$] at 1510 cm^{-1}. Because both these vibrations have dynamic dipoles aligned along the long axis of the naphthalene ring and are quite strong at high coverages (as well as in the pure liquid), the implication is that an adsorption geometry with the ring standing up along its long axis on the surface (with a footprint along the short axis) only develops after exposures above 1.0 L.

In general terms, the RAIRS data indicate that NEA always adsorbs with its aromatic ring perpendicular to or tilted on the surface, even at low coverages. This is consistent with near-edge X-ray absorption fine structure spectroscopy results previously reported by Lambert and co-workers[48] but somewhat surprising in light of the typical behavior seen with aromatic rings on single-crystal metal surfaces, where an initial flat adsorption switches to a tilted arrangement only after reaching a specific threshold coverage.[49−52] Regardless, the nonflat

(39) Lippincott, E. R.; O'Reilly, E. J., Jr. *J. Chem. Phys.* **1955**, *23*, 238.
(40) Chiorboli, P.; Bertoluzza, A. *Ann. Chim.* **1959**, *49*, 245.
(41) Hawkins, J. G.; Ward, E. R.; Whiffen, D. H. *Spectrochim. Acta* **1957**, *10*, 105.
(42) Katritzky, A. R.; Jones, R. A. *J. Chem. Soc.* **1960**, 2942.
(43) Hamada, Y.; Hashiguchi, K.; Hirakawa, A. Y.; Tsuboi, M.; Nakata, M.; Tasumi, M. *J. Mol. Spectrosc.* **1983**, *102*, 123.
(44) Chu, W.; LeBlanc, R. J.; Williams, C. T.; Kubota, J.; Zaera, F. *J. Phys. Chem. B* **2003**, *107*, 14365.
(45) Ma, Z.; Lee, I.; Kubota, J.; Zaera, F. *J. Mol. Catal. A: Chem.* **2004**, *216*, 199.
(46) Lavoie, S.; Laliberté, M.-A.; McBreen, P. H. *J. Am. Chem. Soc.* **2003**, *125*, 15756.
(47) Greenler, R. G. *J. Chem. Phys.* **1966**, *44*, 310.
(48) Bonello, J. M.; Williams, F. J.; Lambert, R. M. *J. Am. Chem. Soc.* **2003**, *125*, 2723.
(49) Hoffmann, H.; Zaera, F.; Ormerod, R. M.; Lambert, R. M.; Wang, L. P.; Tysoe, W. T. *Surf. Sci.* **1990**, *232*, 259.

Table 1. Vibrational Assignments of the Peaks in the RAIRS Data for Pure NEA and for NEA Adsorbed on Platinum Surfaces[a]

	NEA/Pt(111), UHV		NEA/Pt, from CCl_4		
mode	exposure <1.0 L	exposure >1.0 L	(*S*) or (*R*)	racemic	pure liquid
$\delta_{oop}(CH)_{ring\text{-}n}$	865 (w)	865 (s)			861 (s)
$\rho(CH_3)$	920 (m)	922 (m)			917 (m)
$\delta_{oop}(CH)_{ring\text{-}n}$		930 (m)	1102 (vs)	1105 (s)	
$\delta_{ip}(CH)_{ring\text{-}n}$		1121 (s)	1120 (m)	1128, 1132 (w)	1119 (s)
$\delta_{oop}(CH)_{ring\text{-}s}$	1168 (w)	1169 (s)	1162 (m)	1172 (m, br)	1167 (s)
$\delta_{ip}(CH)_{ring\text{-}s}$	1200 (m)	1205 (w)	1198 (m)	1218 (m)	1201 (w)
$\delta_{ip}(CH)_{ring\text{-}n}$		1242 (w)			1242 (w)
$\delta_{ip}(CH)_{ring\text{-}n}$	1257 (m)	1260 (m)	1253 (m)	1253, 1266 (s)	1259 (m)
$\delta(CH)_{EtNH_2}$		1325 (w)	1329 (m)	1323 (m)	1325 (sh)
$\delta(CH)_{EtNH_2}$		1343 (m)	1344 (w)	1345 (m)	1337 (m)
$\delta_s(CH_3)_{EtNH_2}$	1369 (s)	1369 (vs)	1374 (m)		1368 (vs)
$\nu_{ip}(CC)_{ring}$		1396 (m)	1398, 1408 (w)	1403 (m)	1395 (m)
$\delta_a(CH_3)_{EtNH_2}$	1432, 1448 (m)	1446 (s, br)	1443 (w)		1446 (s,br)
$\nu_{ip}(CC)_{ring\text{-}x}$	1510 (w)	1511 (vs)	1520 (vs)	1518, 1578 (s)	1510 (vs)
$\nu_{ip}(CC)_{ring\text{-}y}$	1600 (m)	1597 (vs)	1601 (s)	1598 (s)	1595 (vs)
$\nu_{ip}(CC)_{ring}$	1622 (w)	1620 (sh)	1620 (s)	1618 (s)	
$\nu_s(CH_3)_{EtNH_2}$	2866 (w)	2866 (m)		2870 (m, br)	2867 (m)
$\nu_a(CH_3)_{EtNH_2}$		2922 (m)	2917 (s, br)	2900 (m, br)	2922 (m)
$\nu_{ip,s}(CH)_{ring}$	2970 (vw)	2960 (vs)	2972 (s)	2962, 2972 (w)	2961 (vs)
$\nu_{ip,a}(CH)_{ring}$		3043 (w)	3011, 3032 (m)	3035 (w, br)	3047 (w)
$\nu_{ip,a}(CH)_{ring}$		3059 (m, br)	3065, 3077 (w)	3075 (w, br)	3063 (sh)

[a] All values are reported in cm^{-1}. Modes: ν = stretching, δ = deformation, ρ = rocking. Subindices: ip = in-plane, oop = out-of-plane, s = symmetric, a = asymmetric, $EtNH_2$ = ethylamine moiety, ring = naphthalene ring, ring-n = nonsubstituted benzene side of naphthalene, ring-s = substituted benzene side of naphthalene, ring-*y* = dipole along short axis of naphthalene ring plane, ring-*x* = dipole along long axis of naphthalene ring plane. Intensities: vs = very strong, s = strong, m = medium, w = weak, vw = very weak, sh = shoulder, br = broad.

adsorption of the NEA may have important implications for its ability to impart chirality on surfaces, because tilted adsorption geometries imply smaller footprints and therefore a larger number of remaining unblocked sites on the surface.

The molecular nature of the adsorbate survives to temperatures above ~400 K. TPD experiments indicate stepwise dehydrogenation, with a sharp H_2 peak at ~450 K and broader features at 600 and ~680 K (Figure S4 in the Supporting Information). The first desorption feature amounts to an average of approximately six hydrogen atoms per molecule and can be assigned to complete dehydrogenation of the ethylamine moiety.[48] The remaining hydrogen corresponds to decomposition of the aromatic ring, which is accompanied by desorption of some HCN at ~605 K (Figure S4). Small amounts of molecular nitrogen evolve at 400 and ~900 K, but no C_2N_2 was detected in our experiments, in contrast to previous reports.[48]

3.2. Titration of Chiral Sites Using PO: (a) TPD. The ability of enantiopure NEA to impart enantioselectivity to Pt(111) surfaces was tested next using a chiral titration procedure described in more detail in previous publications.[23,24] In the particular experiments reported here, varying amounts of (*S*)-NEA were first adsorbed on clean Pt(111), and then 2.0 L of either (*S*)- or (*R*)-propylene oxide (PO) was added (all at liquid nitrogen temperatures), after which the desorption of molecular PO was followed by TPD. As indicated in the previous reports,[23,24] PO was chosen as the probe molecule because it desorbs molecularly from these surfaces and can therefore be easily detected and quantified by TPD. Typical TPD traces from these experiments are displayed in Figure 2. Two molecular desorption states [at approximately 185 and 210 K for (*S*)-PO and 180 and 205 K for (*R*)-PO] are evident in these data, and a third, higher-temperature feature [at approximately 230 and 225 K for (*S*)- and (*R*)-PO, respectively] is also seen for low

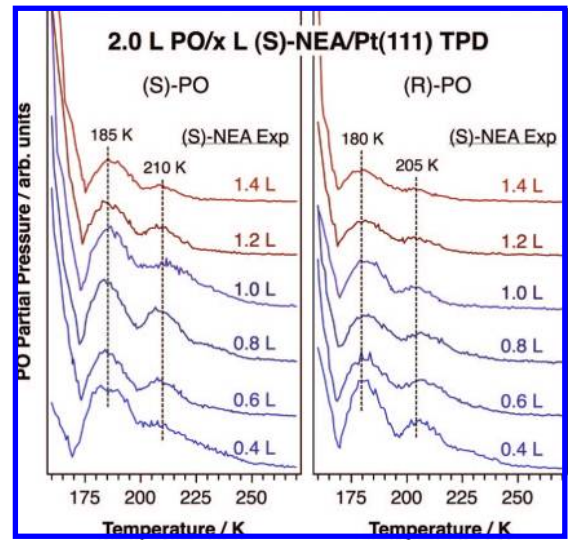

Figure 2. PO-titration TPD traces from Pt(111) surfaces first dosed with various amounts of (*S*)-NEA and then with 2.0 L of either (left) (*S*)- or (right) (*R*)-PO, both at liquid nitrogen temperatures. Two molecular desorption states from monolayer PO adsorption are identified in these data, at approximately 185 and 210 K for (*S*)-PO and at 180 and 205 K for (*R*)-PO.

NEA coverages. All of these states originate from adsorbates in the first layer and saturate at high PO exposures, after which condensation occurs. The condensed PO desorbs at ~145 K (data not shown). Similar results were obtained with (*R*)-NEA: the (*R*)-NEA−(*R*)-PO (RR) pair behaves like the (*S*)-NEA−(*S*)-PO (SS) set and the (*R*)-NEA−(*S*)-PO (RS) pair like the (*S*)-NEA−(*R*)-PO (SR) combination (data not shown).

The appearance of two peaks in the TPD traces in Figure 2 (three at low NEA coverages) argues for the potential strong interaction of adsorbed propylene oxide with adjacent NEA molecules on the surface. Desorption of monolayer PO from either clean or 2-butoxide-covered Pt(111) takes place in a single peak at 195 K.[24] When PO is coadsorbed with 2-methylbutanoic

(50) Netzer, F. P.; Ramsey, M. G. *Crit. Rev. Solid State Mater. Sci.* **1992**, *17*, 397.
(51) Zaera, F. *Chem. Rev.* **1995**, *95*, 2651.
(52) Ma, Z.; Zaera, F. *Surf. Sci. Rep.* **2006**, *61*, 229.

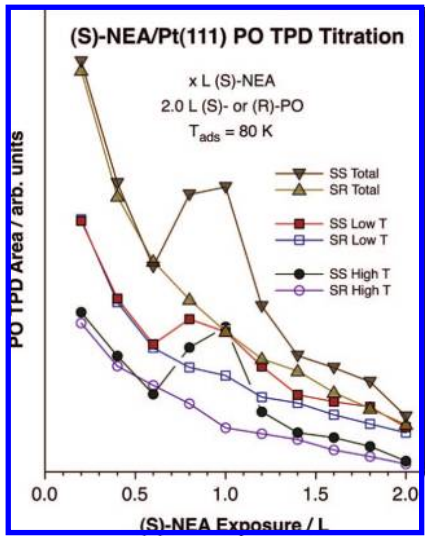

Figure 3. Molecular PO desorption yields, estimated from the TPD titration experiments in Figure 2, as a function of initial (*S*)-NEA exposure. Yields for both low- and high-temperature peaks as well as for the total PO desorption are shown for both (*S*)- and (*R*)-PO adsorbates (i.e., for the SS and SR pairs as defined in the text). A significant enantioselectivity is observed at intermediate NEA exposures (0.6−1.4 L), where the (*S*)-PO yield is significantly higher. This is more noticeable in the high-temperature peak.

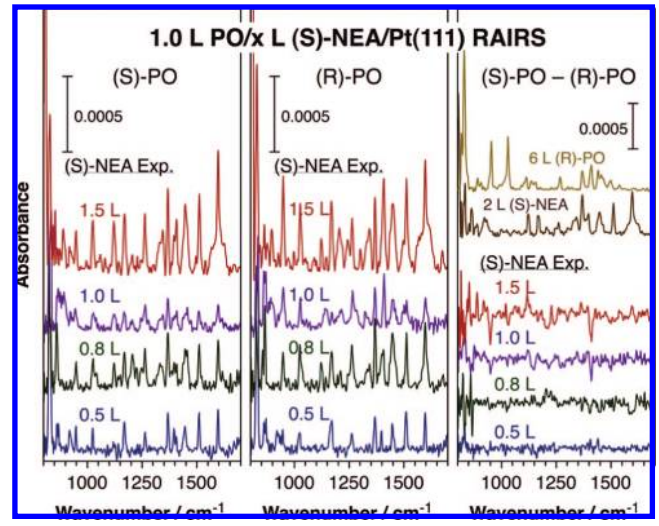

Figure 4. RAIRS from Pt(111) surfaces first exposed to various amounts of (*S*)-NEA and then to 1.0 L of (left) (*S*)- or (middle) (*R*)-PO. The differences between the two sets are highlighted by the (*S*)-PO − (*R*)-PO difference spectra shown in the right panel. Most of those are due to the higher signals obtained for (*R*)-PO, indicating excess adsorption in a specific geometry, but more subtle changes in the adsorbed NEA can also be observed. Spectra for 6.0 L of (*R*)-PO and for 2.0 L of (*S*)-NEA on clean Pt(111) are also provided in the right panel for reference.

acid (2-MBA), a small shift toward higher temperatures (larger for the homochiral 2-MBA + PO pairs) is observed; however, although a distorted peak shape indicative of multiple desorption states is seen in that system, no separate features are apparent.[27] In the case of NEA, the split is quite clear, with the high-temperature state appearing at a temperature ∼25 K higher than that of the regular monolayer peak. Moreover, there is a small but consistent difference between the peak temperatures for (*S*)- and (*R*)-PO: the former always desorbs at higher temperatures with (*S*)-NEA [and at lower temperatures with (*R*)-NEA] than the latter. The temperature difference between the two averages is ∼5 K but changes with NEA coverage (Figure S5 in the Supporting Information), reaching its largest value at the intermediate NEA coverages where the chiral effects are the most noticeable (see below).

The enantioselectivity of NEA-templated Pt(111) toward the adsorption of chiral molecules is indicated by the relative amounts of (*S*)- and (*R*)-PO that can be adsorbed on those surfaces, as extracted from the TPD traces in Figure 2. The areas of those peaks as a function of (*S*)-NEA initial exposure are summarized in Figure 3. A general decrease in PO yields is typically seen as the NEA coverage is increased. However, a deviation from that monotonic trend is seen with (*S*)-PO (the SS pair) at intermediate (*S*)-NEA exposures (approximately 0.6−1.4 L). Also, although that deviation is evident in both the low- and high-temperature peaks, it is more noticeable in the latter. The critical observation here is that such behavior is not seen with the (*R*)-PO enantiomer (the SR pair). This indicates that at these intermediate (*S*)-NEA coverages (estimated to range between half and two-thirds of monolayer saturation), there is a clear enantiopreference for the adsorption of the homochiral PO. This is the type of chiral templating effect that has also been seen with 2-butanol,[24,53] 2-MBA,[26,27] and a number of aminoacids[28] and ascribed to the formation of supramolecular surface structures. The main argument for this interpretation is the coverage dependence observed: the chiral effect is only seen at intermediate coverages of the templating agent.[54]

In summary, the PO-titration TPD experiments provide evidence for both supramolecular templating and individual complexation as possible mechanisms for the way NEA bestows chirality to Pt(111). The fact that the absolute uptakes of the two PO enantiomers differ significantly only at intermediate NEA coverages is a clear indication of a cooperative supramolecular effect, as required by the first mechanism. On the other hand, the observation of a new high-temperature PO desorption state where most of the enantiodifferentiation is observed provides clear evidence for PO−NEA interactions on the surface. The small but consistent shift to higher temperatures seen for the SS and RR pairs compared with the SR and RS pairs also attest to the stronger intermolecular interactions in the former set. Unfortunately, it is not easy to determine the relative extent of the contributions of each of these mechanisms to the overall enantioselectivity on the basis of our data. Finally, it is worth pointing out that the deviation from the regular trends of the PO yields that is seen in the SS and RR cases at intermediate NEA coverages leads to an absolute increase in the total PO uptake compared with that seen at lower NEA coverages. This strongly suggests that the NEA molecules rearrange on the surface in order to make space for the additional PO. Similar behavior has been proposed previously for the case of tartaric acid and methylacetoacetate on Ni(111).[21] This synergistic effect is explored in more detail in the next section.

3.3. Titration of Chiral Sites Using PO: (b) RAIRS. The chirality-bestowing effect of adsorbed NEA on the uptake of PO was also probed by RAIRS. The left and middle panels of Figure 4 show spectra collected for (*S*)- and (*R*)-PO, respectively, coadsorbed with (*S*)-NEA for four different NEA initial exposures, and the right panel displays the differences between

(53) Gao, F.; Wang, Y.; Burkholder, L.; Tysoe, W. T. *J. Am. Chem. Soc.* **2007**, *129*, 15240.

(54) Romá, F.; Stacchiola, D.; Tysoe, W. T.; Zgrablich, G. *Phys. A* **2004**, *338*, 493.

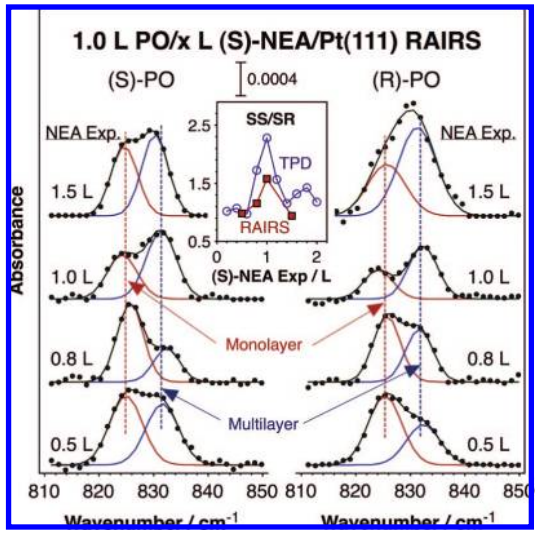

Figure 5. Details of the RAIRS data in Figure 4, highlighting the signals from the ring-deformation mode of PO. Two peaks are seen for that mode at 825 and 832 cm^{-1}, corresponding to monolayer and multilayer adsorption, respectively.[24] In the inset, the ratio SS/SR of the intensities of the monolayer peaks obtained for (*S*)- and (*R*)-PO is plotted as a function of initial (*S*)-NEA exposure (filled squares), showing the enantioselective effect caused by the NEA chiral templating of the surface. Data from the TPD results in Figure 3 (open circles) are also included for comparison.

the two sets of spectra. For reference, spectra are also provided for (*R*)-PO and (*S*)-NEA adsorbed on clean Pt(111).

The most obvious differences between the results for (*S*)-PO versus (*R*)-PO are the larger intensities seen in the latter case for the peaks at 948 and 1412 cm^{-1} for (*S*)-NEA initial doses of 1.0 L or more. These correspond to the methyl rocking [$\rho(CH_3)$] and methylene scissoring [$\gamma(CH_2)$] vibrational modes, respectively, of PO.[24] The frequency values are quite close to those seen in the multilayer, indicating minimal perturbation by interactions with either the adsorbed NEA or the Pt(111) surface. On the other hand, the relative intensities of those modes are quite different from what is observed for the condensed molecules. Particularly noticeable is the absence of signals for the methyl wagging [$\omega(CH_3)$] mode at 1030 cm^{-1} and the methyl deformation [$\delta(CH_3)$] modes at 1369, 1440, and 1457 cm^{-1}, even though all of those are quite strong in the data for PO adsorbed on clean Pt(111). This indicates a molecular orientation with the plane of the ring perpendicular to the surface and the methylene group pointing away from it. It should be noted that the peaks seen in the difference spectra correspond to the additional molecules observed for adsorption of (*R*)-PO as opposed to (*S*)-PO. Adsorbates with a more tilted geometry are indeed evidenced in both cases by the strong signal seen in the individual RAIRS traces for the methyl wagging mode.

Figure 5 provides a detailed view of the region of the spectra in Figure 4 corresponding to the main PO ring-deformation mode. As with other chiral templating agents,[23,24,27] two peaks are seen in this region, due to propylene oxide adsorbed in the first monolayer (~825 cm^{-1}) and in subsequent multilayers (~832 cm^{-1}). The intensity of the peak for the monolayer was used to estimate the magnitude of the enantioselectivity in the PO uptake on (*S*)-NEA-templated surfaces. The inset in Figure 5 summarizes the results from this analysis in the form of the ratio of signal intensities of the 825 cm^{-1} peak for the SS and SR pairs as a function of initial (*S*)-NEA exposure. A clear preference for (*S*)-PO adsorption is indeed identified for (*S*)-NEA exposures of ~1.0 L. The trend observed with RAIRS follows quite nicely that seen in the PO TPD titration experiments reported above (also plotted in the Figure 5 inset for reference). The SS/SR ratios appear to be smaller in the RAIRS experiments, but that may be explained by potential changes in adsorption geometry, which also affect the absolute intensity of the RAIRS peaks.

As mentioned above, the most salient differences between the RAIRS of the coadsorbed (*S*)-NEA + (*S*)- or (*R*)-PO in Figure 4 are those associated with the adsorbed PO itself. Nevertheless, some changes are also apparent in the peaks associated with the adsorbed (*S*)-NEA species. For one, the RAIRS data from the NEA-preexposed Pt(111) surfaces display more intense NEA peaks after PO saturation than before PO exposure, an increase equivalent to ~0.2 L higher (*S*)-NEA doses. Surprisingly, though, this change is less marked at intermediate NEA coverages, where the enantioselectivity for PO adsorption is the most noticeable. Moreover, the peaks near 1370 cm^{-1} due to the methyl umbrella mode appear to be less intense than the rest, suggesting a flat orientation for the methyl group. Unfortunately, no clear peak-frequency shifts are seen at any coverages, and the signal intensities are too weak to reach any definitive conclusions regarding possible intermolecular interactions between the NEA and PO surface species. All that can be said here is that there appears to be a synergistic effect by which the added PO induces a molecular rearrangement of the NEA on the surface, perhaps forcing the molecules to adopt a more upright configuration with a smaller footprint, and that the extent of that effect depends on coverage and the type of chiral pairing involved (SS vs SR or, equivalently, RR vs RS). This effect is likely to be common to other coadsorbates, perhaps even to the α-ketoesters typically used as reactants in cinchona-modified hydrogenation catalysts, although it is clear that the specifics of each system do matter. Unfortunately, the behavior of adsorbed NEA in the presence of coadsorbed ethyl pyruvate (EtPy) could not be tested by titration experiments such as the ones performed with PO because the pyruvate dehydrogenates extensively rather than desorbing molecularly under vacuum. Instead, that chemistry was tested by RAIRS in situ in the presence of a solvent to better mimic real catalytic conditions (see below).

3.4. Room-Temperature NEA Uptake from CCl_4 Solutions. Finally, the uptake of NEA from solution onto platinum surfaces was probed in situ by RAIRS. Our previous work with cinchona alkaloids and related compounds has highlighted the importance of testing the adsorption of these compounds in the presence of the solvent; otherwise, decomposition on the surface even below room temperature is likely.[37,45,55] Significant changes in the RAIRS spectra with the solvent compared with those obtained for the pure compounds or for the adsorbates under UHV conditions are also typically observed. The CCl_4 solvent is inert and does not react with the surface or the other molecules,[55,56] but it clearly affects the environment surrounding the adsorbates.[37,57] The in-situ experiments in the presence of a solution of the reactants also allows for reversible adsorption,[37,58] which is not viable under vacuum. Indeed, differences in the adsorbate in the presence of a solution versus under vacuum are seen in the case of NEA, as indicated by the data reported in Figure 6, which displays the spectra for (*S*)-, (*R*)-, and racemic

(55) Ma, Z.; Zaera, F. *J. Phys. Chem. B* **2005**, *109*, 406.
(56) Ma, Z.; Zaera, F. *Catal. Lett.* **2004**, *96*, 5.
(57) Mink, L.; Ma, Z.; Olsen, R. A.; James, J. N.; Sholl, D. S.; Mueller, L. J.; Zaera, F. *Top. Catal.* **2008**, *48*, 120.
(58) Ma, Z.; Zaera, F. *J. Am. Chem. Soc.* **2006**, *128*, 16414.

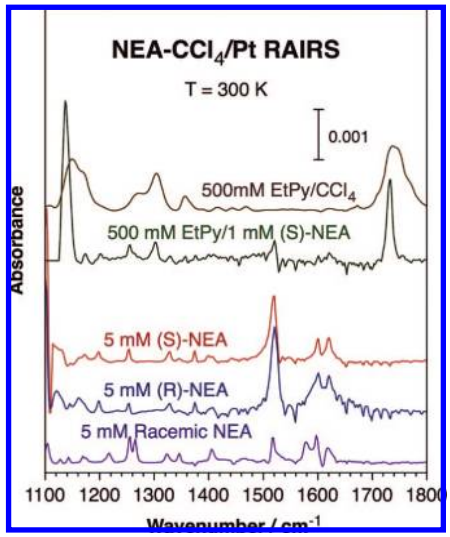

Figure 6. In-situ RAIRS spectra for (*S*)-, (*R*)-, and racemic NEA adsorbed from 5 mM CCl_4 solutions onto a polished polycrystalline platinum surface at room temperature (bottom three traces). In particular, the differences between the trace for the racemic mixture and the other two should be noticed. The second trace from the top corresponds to a surface exposed sequentially to 1 mM (*S*)-NEA and 500 mM EtPy CCl_4 solutions. The top trace corresponds to a surface exposed only to a 500 mM EtPy solution and is provided for reference.

NEA adsorbed on a polished polycrystalline platinum surface from the corresponding 5 mM CCl_4 solutions. Vibrational assignments for these data are provided in Table 1.

One noticeable observation from the (*S*)- and (*R*)-NEA RAIRS data in Figure 6 is the predominance of the peak for the in-plane ring deformation along the long axis [$\nu_{ip}(CC)_{ring\text{-}x}$], which here (when adsorbed from solution) is seen at 1520 cm^{-1}. Since the feature for the ring deformation along the short axis [$\nu_{ip}(CC)_{ring\text{-}y}$ at 1601 cm^{-1}] is significantly less intense, it is clear that adsorption occurs with the naphthalene ring standing on its short side. Other in-plane modes are also detected in the spectra, specifically the C−H deformations [$\delta_{ip}(CH)_{ring}$] at 1198 and 1253 cm^{-1}, supporting the idea that the ring is essentially perpendicular to the plane of the surface. On the other hand, modes with dipole components perpendicular to the ring, including the out-of-plane C−H deformation [$\delta_{oop}(CH)_{ring\text{-}s}$] at 1162 cm^{-1} and the methyl symmetric deformation [$\delta_s(CH_3)_{EtNH_2}$] at 1372 cm^{-1}, are also seen, so a degree of tilting is apparent. The adsorption geometry adopted by NEA can be associated with that seen for cinchonine and is different from that adopted by cinchonidine.[57] This is an interesting observation because both NEA and cinchonine are less enantioselective than cinchonidine in catalytic hydrogenation reactions;[59−61] perhaps the unique ability of cinchonidine to adopt a different adsorption arrangement contributes to its particularly good behavior as chiral modifier in catalysis. One additional important behavior identified here is the fact that the adsorption geometry of NEA does not seem to change as a function of surface coverage: similar spectra (albeit with different absolute peak intensities) were obtained using solutions having different concentrations of either (*S*)- or (*R*)-NEA (Figures S6 and S7 in the Supporting Information). This is in contrast to the changes in adsorption geometry observed with cinchona alkaloids under similar circumstances.[37,44,62]

Another interesting observation worth highlighting from the data in Figure 6 is the significant differences observed in the RAIRS obtained for a racemic mixture of NEA. Most noticeable is the splitting of some of the vibrational features, including those for the in-plane C−H deformations in the nonsubstituted ring of the naphthalene moiety [$\delta_{ip}(CH)_{ring\text{-}n}$], which are seen at 1253 cm^{-1} for all three NEAs but also at 1266 cm^{-1} for the racemic mixture, and the in-plane ring deformation [$\nu_{ip}(CC)_{ring\text{-}x}$] observed at 1518 and 1578 cm^{-1} for the racemic mixture. This type of splitting is common in the solid state when molecules occupy nonequivalent sites in the crystal lattice and here suggests a potential intermolecular (*S*)-NEA + (*R*)-NEA pairing on the surface. Such behavior is somewhat surprising because adsorption of racemic mixtures on surfaces typically leads to segregation into homochiral domains, at least under vacuum.[63,64] Also worthy of notice is the fact that the molecular adsorption geometry seen for the adsorbed NEA obtained from the racemic mixture is different than that seen with the pure enantiomers: the relatively large signals for the peaks at 1403 and 1598 cm^{-1}, corresponding to $\nu_{ip}(CC)_{ring\text{-}y}$ modes, indicate a ring oriented with its long axis nearly parallel to the surface. As in the case of the pure enantiomers, this adsorption geometry was observed for all of the solution concentrations tried (Figure S8 in the Supporting Information).

Finally, the coadsorption of NEA with EtPy, a typical reactant in chiral α-ketoester hydrogenation catalysis, was briefly explored. The second-from-the-top trace in Figure 6 corresponds to a surface exposed first to a 1 mM solution of (*S*)-NEA and then to a 500 mM solution of EtPy, both in CCl_4. It would appear at first sight that the resulting RAIRS may be equivalent to the sum of the spectra for each individual adsorbate. This is further suggested by the progressive growth of the peaks due to EtPy as the concentration of that solution is increased (Figure S9 in the Supporting Information). However, the peaks for the EtPy adsorbate in the presence of NEA (Figure 6, second trace from the top) are sharper and slightly red-shifted from those seen when EtPy is adsorbed on clean platinum (Figure 6, top trace). Some red-shifting can be seen as a function of concentration with EtPy alone (Figure S10 in the Supporting Information), but that cannot account for the full ∼5 cm^{-1} shifts seen here. It does appear that the presence of adsorbed NEA on the surface modifies the adsorption of EtPy, perhaps inducing more order and some degree of intermolecular vibrational coupling. However, no clear evidence for direct intermolecular bonding between NEA and EtPy on the surface could be detected within the experimental errors of our technique.

4. Conclusions

In this report, we have summarized the results obtained from reflection absorption infrared spectroscopy (RAIRS) and temperature-programmed desorption (TPD) experiments aimed to characterize the ability of 1-(1-naphthyl)ethylamine (NEA) to bestow chirality on platinum surfaces. Chiral titration experiments under ultrahigh vacuum using propylene oxide (PO) indicate a preference for the uptake of one enantiomer (the one

(59) Simons, K. E.; Meheux, P. A.; Ibbotson, A.; Wells, P. B. *Stud. Surf. Sci. Catal.* **1993**, *75*, 2317.
(60) Blaser, H.-U.; Jalett, H. P.; Lottenbach, W.; Studer, M. *J. Am. Chem. Soc.* **2000**, *122*, 12675.
(61) Meier, D. M.; Mallat, T.; Ferri, D.; Baiker, A. *J. Catal.* **2006**, *244*, 260.
(62) Kubota, J.; Zaera, F. *J. Am. Chem. Soc.* **2001**, *123*, 11115.
(63) Ernst, K. H. *Top. Curr. Chem.* **2006**, *265*, 209.
(64) Barlow, S. M.; Raval, R. *Curr. Opin. Colloid Interface Sci.* **2008**, *13*, 65.

with the same chirality as the adsorbed NEA) over the other. This only occurs at intermediate NEA surface coverages, a behavior that has traditionally been ascribed to the formation of supramolecular surface structures with chiral empty pockets (also known as surface templating). On the other hand, a strong interaction between the adsorbed NEA and PO molecules, slightly stronger for the homochiral pairs, is seen in TPD experiments. This suggests a mechanism by which chirality is imparted to the surface via a direct one-to-one modifier−reactant (NEA−PO) interaction. The enantioselective uptake of PO by the NEA-modified platinum surfaces is accompanied by changes in adsorption geometry, implying that the surface modification is not static and that there is a synergy between the modifier and the probe molecule or the reactant.

The uptake of NEA onto platinum surfaces from carbon tetrachloride solutions also points to the relevance of the chirality of the molecules in the adsorption process. In particular, significantly different RAIRS data are obtained with enantiopure versus racemic NEA. It appears that the (*S*) and (*R*) enantiomers of NEA in the racemic case may pair up and force the formation of a very different layer than that obtained with either enantiomer alone. Moreover, the addition of ethyl pyruvate (EtPy) on NEA-precovered Pt surfaces leads to its adsorption in a unique and ordered fashion not seen when the dosing is done on the clean substrate. Although no direct spectroscopic evidence was obtained for intermolecular interactions between NEA and the second chiral adsorbate in the case of PO under vacuum or EtPy from solution, a synergy was identified in both cases via the detection of changes in adsorption geometries. It appears that both supramolecular templating and one-to-one complexation contribute to the behavior of NEA as a chiral modifier on platinum surfaces. More generally, it is possible that all chiral modification systems involve a combination of entropic and enthalpic factors and should not be described exclusively in terms of one of these factors or the other.

One last word of caution: chiral modification by NEA, cinchona alkaloids, and other related compounds in catalysis has proven to be the result of a delicate balance among several factors, including the nature of the surface,[65,66] the pretreatment of the catalyst,[67−69] the solvent,[55,70,71] the concentration of the modifier,[62,72,73] the presence of acidic functions,[74] and the reaction temperature,[75,76] among others.[37,58,59,77,78] Certainly, the conditions used in the studies reported here are somewhat different than those used in catalysis. The experiments using the in situ RAIRS setup, where the surface is exposed to a liquid phase (and to hydrogen), are closer to the real systems, but additional work using more relevant solvents is still needed. Our results need to be placed in this broader context and the conclusions considered accordingly. It is also interesting to note that protonation of the cinchona[68,79] or NEA[80] modifiers may be required for highly enantioselective behavior to occur. Protonation can also change the molecular configuration of the modifier,[57,81] thereby affecting the way it adsorbs on the surface.[82]

Acknowledgment. Funding for this project was provided by the U.S. Department of Energy.

Supporting Information Available: Uptake RAIRS for (*R*)- and racemic (commercial and homemade) NEA on Pt(111) at 80 K and under UHV; TPD of (*S*)-NEA on Pt(111); peak temperatures from (*R*)- and (*S*)-PO titrations of (*S*)-NEA/Pt(111) surfaces; uptake RAIRS for (*S*)-, (*R*)-, and racemic NEA from CCl_4 solutions on a Pt polished disk at 295 K; RAIRS for (*S*)-NEA on Pt after exposure to different concentrations of EtPy in CCl_4; and uptake RAIRS for EtPy from CCl_4 solutions on a Pt polished disk at 295 K. This material is available free of charge via the Internet at http://pubs.acs.org.

JA803667V

(65) Wehrli, J. T.; Baiker, A.; Monti, D. M.; Blaser, H. U. *J. Mol. Catal.* **1989**, *49*, 195.
(66) Attard, G. A.; Griffin, K. G.; Jenkins, D. J.; Johnston, P.; Wells, P. B. *Catal. Today* **2006**, *114*, 346.
(67) Meheux, P. A.; Ibbotson, A.; Wells, P. B. *J. Catal.* **1991**, *128*, 387.
(68) Minder, B.; Mallat, T.; Skrabal, P.; Baiker, A. *Catal. Lett.* **1994**, *29*, 115.
(69) Schurch, M.; Schwalm, O.; Mallat, T.; Weber, J.; Baiker, A. *J. Catal.* **1997**, *169*, 275.
(70) Wehrli, J. T.; Baiker, A.; Monti, D. M.; Blaser, H. U.; Jalett, H. P. *J. Mol. Catal.* **1989**, *57*, 245.
(71) Bartók, M.; Sutyinszki, M.; Balázsik, K.; Szöllodblacsi, G. *Catal. Lett.* **2005**, *100*, 161.
(72) Bond, G.; Simons, K. E.; Ibbotson, A.; Wells, P. B.; Whan, D. A. *Catal. Today* **1992**, *12*, 421.
(73) Blaser, H. U.; Garland, M.; Jallet, H. P. *J. Catal.* **1993**, *144*, 569.
(74) von Arx, M.; Mallat, T.; Baiker, A. *J. Mol. Catal. A: Chem.* **1999**, *148*, 275.
(75) Sutherland, I. M.; Ibbotson, A.; Moyes, R. B.; Wells, P. B. *J. Catal.* **1990**, *125*, 77.
(76) LeBlanc, R. J.; Williams, C. T. *J. Mol. Catal. A: Chem.* **2004**, *220*, 207.
(77) Singh, U. K.; Landau, R. N.; Sun, Y.; LeBlond, C.; Blackmond, D. G.; Tanielyan, S. K.; Augustine, R. L. *J. Catal.* **1995**, *154*, 91.
(78) Wang, J.; Sun, Y.; LeBlond, C.; Landau, R. N.; Blackmond, D. G. *J. Catal.* **1996**, *161*, 752.
(79) Schwalm, O.; Minder, B.; Weber, J.; Baiker, A. *Catal. Lett.* **1994**, *23*, 271.
(80) Minder, B.; Schürch, M.; Mallat, T.; Baiker, A. *Catal. Lett.* **1995**, *31*, 143.
(81) Olsen, R. A.; Borchardt, D.; Mink, L.; Agarwal, A.; Mueller, L. J.; Zaera, F. *J. Am. Chem. Soc.* **2006**, *128*, 15594.
(82) Vargas, A.; Ferri, D.; Baiker, A. *J. Catal.* **2005**, *236*, 1.